EJA

Eur J Anaesthesiol 2022; **39:**758–765

ORIGINAL ARTICLE

Artificial intelligence using deep neural network learning for automatic location of the interscalene brachial plexus in ultrasound images

Xiao-Yu Yang*, Le-Tian Wang*, Gen-Di Li*, Ze-Kuan Yu, Dong-Li Li, Qing-Lai Guan, Qing-Rong Zhang, Ting Guo, Hai-Lian Wang and Ying-Wei Wang

BACKGROUND Identifying the interscalene brachial plexus can be challenging during ultrasound-guided interscalene block.

OBJECTIVE We hypothesised that an algorithm based on deep learning could locate the interscalene brachial plexus in ultrasound images better than a nonexpert anaesthesiologist, thus possessing the potential to aid anaesthesiologists.

DESIGN Observational study.

SETTING A tertiary hospital in Shanghai, China.

PATIENTS Patients undergoing elective surgery.

INTERVENTIONS Ultrasound images at the interscalene level were collected from patients. Two independent image datasets were prepared to train and evaluate the deep learning model. Three senior anaesthesiologists who were experts in regional anaesthesia annotated the images. A deep convolutional neural network was developed, trained and optimised to locate the interscalene brachial plexus in the ultrasound images. Expert annotations on the datasets were regarded as an accurate baseline (ground truth). The test dataset was also annotated by five nonexpert anaesthesiologists.

MAIN OUTCOME MEASURES The primary outcome of the research was the distance between the lateral midpoints of the nerve sheath contours of the model predictions and ground truth.

RESULTS The data set was obtained from 1126 patients. The training dataset comprised 11 392 images from 1076 patients. The test dataset constituted 100 images from 50 patients. In the test dataset, the median [IQR] distance between the lateral midpoints of the nerve sheath contours of the model predictions and ground truth was 0.8 [0.4 to 2.9] mm: this was significantly shorter than that between nonexpert predictions and ground truth (3.4 mm [2.1 to 4.5] mm; $P < 0.001$).

CONCLUSION The proposed model was able to locate the interscalene brachial plexus in ultrasound images more accurately than nonexperts.

TRIAL REGISTRATION ClinicalTrials.gov (https://clinicaltrials.gov) identifier: NCT04183972.

Published online 20 July 2022

KEY POINTS

- A deep learning model was developed to identify the interscalene brachial plexus in ultrasound images.
- The model was trained with over 10 000 ultrasound images from more than 1000 patients.
- The model can locate the interscalene brachial plexus better than nonexpert anaesthesiologists.

Introduction

Peripheral nerve blocks have gained widespread popularity because of their benefits both as a valuable alternative to general anaesthesia and as a preferred modality for postoperative pain management.[1,2] One of the essential steps for achieving a successful peripheral nerve

* Xiao-Yu Yang, Le-Tian Wang, Gen-Di Li contributed equally to the study.

From the Department of Anaesthesiology, Huashan Hospital Fudan University (X-YY, L-TW, D-LL, Q-LG, Q-RZ, TG, H-LW, Y-WW), Department of Surgery Nursing, Huashan Hospital Fudan University (G-DL) and the Academy for Engineering and Technology, Fudan University, Shanghai, China (Z-KY)

Correspondence to Ying-Wei Wang, Professor, Department of Anaesthesiology, Huashan Hospital Fudan University, Shanghai, China
E-mail: wangyw@fudan.edu.cn

DOI:10.1097/EJA.0000000000001720

block is to localise the target nerves.[3] Ultrasound has undoubtedly become the current mainstream technique for localising nerves as it enables the direct visualisation of the targeted nerves and adjacent anatomical structures in real time.[2–4] Nevertheless, a successful ultrasound-guided nerve block is not easy to achieve.[3]

Whenever performing an interscalene brachial plexus block, it can sometimes be challenging for anaesthesiologists, especially inexperienced ones, to identify the nerve elements of the brachial plexus between the scalene muscles in ultrasound images.[5] In ultrasound images, the shape, position and echogenicity of these nerves varies remarkably, both along their course and from patient to patient.[3,6] Additionally, ultrasound images are intrinsically vague, with limited resolution, multiple artifacts and noise.[7] Incorrect recognition of the interscalene brachial plexus during an attempted block might be frequent. In a study of interscalene and supraclavicular block, the combined incidence of unintentional intraneural injection under ultrasound guidance was reported as 17%.[8] Therefore, assisting anaesthesiologists to locate the interscalene brachial plexus in ultrasound images might be of clinical value. To date, only a few computer programmes have been developed for localising nerves during ultrasound guidance, and their clinical value is uncertain.[9–11]

The rapidly evolving artificial intelligence computer technology has heralded a new era in the practice of anaesthesiology.[12] The use of artificial intelligence, mainly machine learning, has achieved remarkable successes in many clinical settings, especially in medical image analysis[13] and clinical predictions.[14] 'Deep learning' is a subset of machine learning that is widely used[15]: it is the technique underpinning AlphaGo, self-driving cars and several medical algorithms that are reported to surpass the performance of physicians.[16] In a study of automatic detection of malignant pulmonary nodules in chest radiographs, an algorithm based on deep learning outperformed physicians in the classification of radiographs and nodule detection, and it enhanced the physicians' performance when used as a second reader.[17]

We hypothesised that a deep learning approach based on convolutional neural networks could locate the interscalene brachial plexus in ultrasound images with better accuracy than nonexpert anaesthesiologists.

Methods

The study design was reviewed and approved by the institutional ethics committee of Huashan Hospital, Fudan University, Shanghai, China on 8 November 2019. The protocol number was KY2019-502.

Ultrasound images and videos were collected from 1126 patients scheduled for elective surgery at Huashan Hospital from January 2019 to September 2020: data from 411 patients were collected retrospectively and from 715 patients prospectively. Written informed consent was obtained from all participants except for seven retrospectively enrolled patients who could not be contacted. This exemption from a requirement for informed consent was permitted by the institutional ethics committee. The inclusion criteria were adult patients aged, 18 to 80 years, ASA physical status class I or II and scheduled for elective surgery for any procedure. Exclusion criteria were skin lesions or infection of the neck, known peripheral neuropathy, history of brachial nerve plexus injury, previous injury or operation in the neck, pregnancy or breastfeeding or allergy to ultrasound gel. The study was registered in ClinicalTrials.gov (https://clinicaltrials.gov) prior to patient enrollment, ID: NCT04183972.

Prospective data collection was performed in the operating room before surgery. Patient identification, gender, age, height and weight were recorded before data collection. Patients were in the supine position, with the head turned slightly away from the anaesthesiologist, and both arms lay by the side of the body. The right interscalene brachial plexus was visualised using a high-frequency probe of an ultrasound system (Sonosite EDGE, manufactured by Fujifilm Inc., Washington, USA, or GE LOGIQ e, manufactured by General Electric Company, Massachusetts, USA). Subsequently, images and videos (about 10 s duration), tracing the brachial plexus course from the interscalene level to the supraclavicular level were captured and saved. The same procedure was followed to collect images and videos of the interscalene brachial plexus in the left side of the neck. To save research costs and time, existing ultrasound images and/or videos of the interscalene brachial plexus in the departmental database were also used. These had been collected by qualified anaesthesiologists using the same ultrasound systems and procedures as for prospective patients. These retrospective data were originally collected, with patient consent, for educational purpose between January and October in 2019 from adult patients undergoing elective surgery. We evaluated eligibility of these patients on the basis of their medical records.

Training dataset preparation and annotation

We extracted a video frame every 0.5 s, thus some 20 images were obtained from each video. For retrospective data without videos, all available images were used. All images were anonymised before their inclusion in the dataset. We randomly sampled 12 (6 from each side) images of almost every patient to construct the training dataset: if 12 images were not available, all the suitable images were used. After deleting invalid images (mainly corrupt files), approximately 12 000 images from 1076 patients were prepared for annotation. To enable the artificial intelligence model to learn, it was necessary that the correct location of the interscalene brachial plexus in these images be outlined. The accuracy of these annotated outlines in the training data was essential for

optimal model performance. Therefore, three senior anaesthesiologists who had received specific training on how to annotate ultrasound images manually outlined the brachial plexus on the images using Photoshop 10.0 (Adobe, San Jose, USA). These expert anaesthesiologists were specialised in anaesthesia for orthopaedic surgery and experienced in interscalene block, with success rates higher than 95%. The experts annotated the images by manually outlining the nerve sheath of the interscalene brachial plexus. Only images with annotations agreed by all three experts were included in the training dataset, otherwise the image was discarded and another image was used from the same side of the neck of the same patient. The detailed annotation process is described in the supplement (supplement.doc, http://links.lww.com/EJA/A747). The workflow of the study is illustrated in Fig. 1.

After the training dataset had been constructed, 100 images from 50 patients (1 image from each side of the neck at any position between the C5 and C7 levels) were collected to construct the test dataset. The test dataset was completely independent of the training dataset. The same group of three expert anaesthesiologists completed the annotation procedures in the same manner as described for the training dataset. These expert annotations indicating the location where the interscalene brachial plexus actually existed in each image in the test dataset were regarded as the 'ground truth'.

Considering the various shapes, positions and echogenicity of the brachial plexus at interscalene level, the deep convolutional neural network was our optimal choice of artificial intelligence technique for locating the brachial plexus in ultrasound images. Thus, a convolutional neural network was developed and trained to locate the interscalene brachial plexus in ultrasound images (Supplemental Fig. 1 Overview, http://links.lww.com/EJA/A739; Supplemental Fig. 2 ResNet, http://links.lww.com/EJA/A740). The input was ultrasound images with or without the presence of the interscalene brachial plexus. The output was a predicted location of the interscalene brachial plexus in these ultrasound images. Supplemental Figure 3, http://links.lww.com/EJA/A741 (supplement.doc, http://links.lww.com/EJA/A747) illustrates a typical example of the image processing flow from an input image to an output prediction result. The detailed model preparation processes are also presented in Supplements (supplement.doc, http://links.lww.com/EJA/A747).

Statistical analysis

The output of the trained model for the test dataset was used to evaluate its performance by comparing the predicted location with the ground truth in each image.

The primary outcome of the research was the distance between model predictions and ground truth of the midpoint of the lateral nerve sheath contour. The brachial nerve root C6 is often used as the starting point of injection during interscalene block,[18] so we calculated the midpoint of the lateral side of the nerve sheath and used this to represent the C6 level (Supplemental Figure 4, http://links.lww.com/EJA/A742). We assumed that a distance less than 1 mm was clinically undiscernible, and thus acceptable, and a distance at least 1 mm indicated an error in defining the nerve sheath at the C6 level. Secondary outcomes were the intersection over union (IoU), and the sensitivity and specificity in detecting the presence of the interscalene brachial plexus in the images.

IoU and F1 score evaluate the location agreement of two regions.[19] Their values range from 0 to 100% (0 to 1) (Supplemental Figure 5, http://links.lww.com/EJA/A743). A higher value indicates a better location agreement (Supplemental Figure 6, http://links.lww.com/EJA/A744). The average symmetric surface distance (ASSD) and Hausdorff distance are measures evaluating the distance between the contours of two regions[19] (Supplemental Figure 7, http://links.lww.com/EJA/A745). Smaller distances indicate better contour proximity. Detailed explanations of these measures are included in the Supplement (Evaluation measures, http://links.lww.com/EJA/A747).

The test dataset was also annotated separately by five attending anaesthesiologists who were neither members of the research group nor specialised in orthopaedic anaesthesia: these anaesthesiologists had completed training in ultrasound-guided regional anaesthesia during their residency but rarely performed interscalene blocks in their current practice. They were trained on how to manually delineate the outer margin of the brachial plexus sheath in ultrasound images. If they identified the brachial nerve roots but had difficulty in discerning the nerve sheath, they were encouraged to guess and delineate the sheath rather than leave the image blank to improve their performance. The performance of these nonexpert anaesthesiologists was evaluated by comparing their predictions to the ground truth using the same set of measures. The results of nonexpert anaesthesiologists and the trained model were also compared.

Patient characteristics data are presented as mean ± SD or number (%). Results are presented as median [IQR or range] or percentage [95% confidence interval (CI)]. The 95% CIs of proportions were calculated using the exact binomial method. The statistical analysis was performed using Stata 15.1 (StataCorp LLC Texas, USA). Continuous outcomes (i.e. the distance between the model prediction and ground truth for both the lateral and medial contour midpoints, ASSD, Hausdorff distance and IoU) were compared between the model and nonexpert anaesthesiologists using the paired Wilcoxon test. Fisher's exact test was used to compare nominal outcomes between the model prediction and averaged nonexpert anaesthesiologists (i.e. accuracy, sensitivity and

Fig. 1 Preparation of the datasets and study workflow.

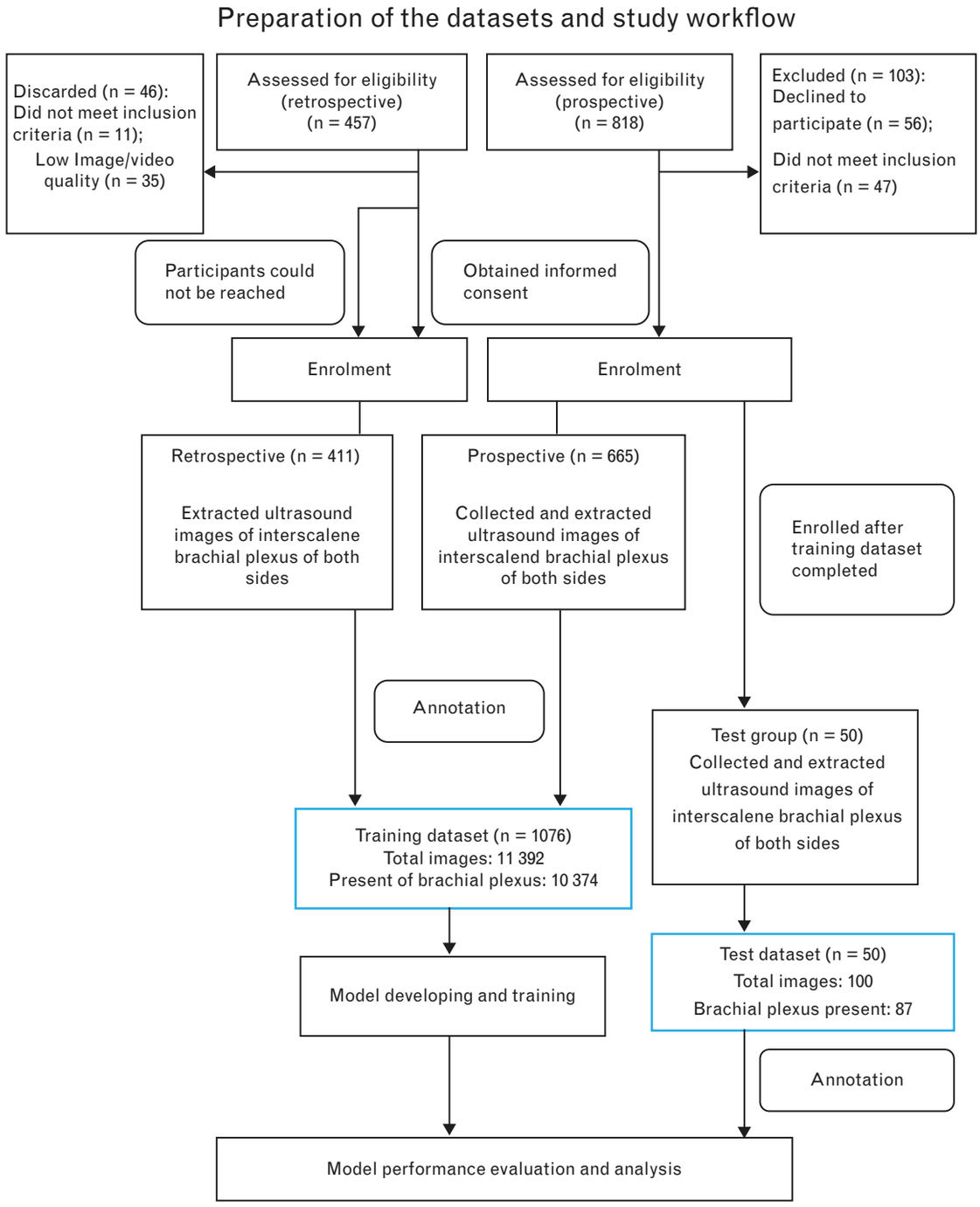

specificity rates in detecting the presence of the brachial plexus). For all tests, a *P* value less than 0.05 was considered statistically significant.

Results

A total of 1126 patients (411 retrospective and 715 prospective patients) were included in the study. Table 1 shows the characteristics of the patients and the images. No image from the same patient was in both the training dataset and the testing dataset.

The trained network achieved an accuracy of 96 (95% CI, 90.1 to 98.9)%, with a sensitivity of 97.7% and a specificity of 84.6% for identifying the presence of the interscalene

Table 1 Patients' and dataset characteristics

	Training set ($n = 1076$)	Test set ($n = 50$)
Patient characteristics		
Age (years)	50 ± 15	50 ± 18
Sex		
Female	449 (42%)	11 (22%)
Male	627 (58%)	39 (78%)
Height (cm)	167 ± 8	171 ± 8
Weight (kg)	66 ± 11	70 ± 12
BMI (kg m^{-2})	23.40 ± 3.27	23.94 ± 2.82
Image set characteristics		
Number of images	11392	100
Brachial plexus present	10374 (91%)	87 (87%)
Brachial plexus absent	1018 (9%)	13 (13%)

Data are mean ± SD, *n*, *n* (%).

brachial plexus in ultrasound images of the test dataset (Table 2). The accuracy of the model is comparable to that of the averaged nonexpert anaesthesiologists (96 vs. 92%, $P = 0.373$).

The nerve location results of the model and nonexpert anaesthesiologists are listed in Table 2. The median distance of the lateral midpoints of the nerve sheath contour between model predictions and the ground truth was significantly less than that between the predictions of nonexpert anaesthesiologists and the ground truth (0.8 vs. 3.4 mm, $P < 0.001$). The median IoU of nonexpert anaesthesiologists' predictions and ground truth was also significantly lower than that achieved by the model ($P < 0.001$). The model achieved a mean F1 score of 0.802, whereas the mean F1 score of the nonexpert anaesthesiologists was 0.630. Figure 2 shows two representative images from the test dataset with expert annotations, model predictions and predictions of the five nonexpert anaesthesiologists.

Discussion

Our study demonstrates that a trained convolutional neural network can locate the interscalene brachial plexus in ultrasound images with better accuracy than nonexpert anaesthesiologists.

In computer artificial intelligence, the convolutional neural network is the current state of the art for automatically learning image patterns and relationships from existing images to correctly recognise patterns in future unseen images.[12] Studies on medical imaging demonstrate that convolutional neural networks have achieved physician-level or even better accuracy in several identification and classification tasks.[17,20–22] Several convolutional neural network-based algorithms for localising nerves in ultrasound images have been reported. Huang *et al.* utilised a convolutional neural network to locate the region of the femoral nerve.[23] They used 562 ultrasound images for training, validation and testing. Their model achieved a median IoU of 64.4 [55.5 to 73.5)% in the test dataset: the accuracy of nerve location in the test set was 83.9%, assuming that an IoU greater than 50% could be defined as accurate.[23] Smistad *et al.*[24] applied a convolutional neural network to identify the location of axillary brachial nerves. They collected a dataset of 462 images from 49 individuals. According to their results, the median and ulnar nerves were easy to detect (*F* score of 0.73 and 0.62, respectively), whereas the detection of the radial nerve was the hardest task (*F* score = 0.39).[24] These researchers focused on improving convolutional neural network algorithms and testing different techniques rather than evaluating the clinical relevance of such an approach using an independent data set. Therefore, the potential clinical capability of convolutional neural networks in locating nerves has not been assessed.

Our proposed model integrates recent advances in deep learning techniques and was specifically adjusted for the ultrasound image nerve identification task. The training dataset consisted of 11 392 images from 1076 participants. This is a much larger dataset than either of the above

Table 2 Results of the model and the average of nonexpert anaesthesiologists on the test dataset

	Model	Anaesthesiologists' average	*P*
Identify the presence of the interscalene brachial plexus ($n = 100$)			
Sensitivity (%)	97.7 (91.4 to 99.7)	95.4 (88.6 to 98.7)	0.682
Specificity (%)	84.6 (54.6 to 98.1)	61.5 (31.6 to 86.1)	0.378
Identify the location of the interscalene brachial plexus ($n = 87$)			
Median distance[a]			
Lateral side (mm)	0.8 [0.4 to 2.9]	3.4 [2.1 to 4.5][b]	<0.001
Medial side (mm)	0.8 [0.4 to 2.9]	3.3 [2.2 to 4.1][a]	<0.001
ASSD (mm)	0.4 [0.3 to 0.8]	1.3 [1.0 to 1.6][a]	<0.001
Hausdorff distance (mm)	1.5 [1.1 to 5.0]	5.9 [4.3 to 7.5][a]	<0.001
Intersection over union (%)	81.2 [63.6 to 85.3]	51.2 [44.0 to 57.2][a]	<0.001
Intersection over union (%) distribution			
>80%	47 (54.0%)	0 (0%)	
50 to 80%	24 (27.6%)	48 (55.2%)	
20 to 50%	16 (18.4%)	39 (44.8%)	
<20%	0 (0%)	0 (0%)	

Data are presented as percentage (95% CI), number (%) or median [IQR]. ASSD, average symmetric surface distance. [a] The median distance between the midpoint of the lateral/medial boundaries of the ground truth annotation and those of model and between the ground truth and average annotations of 5 inexperienced anaesthesiologists. [b] *P* less than 0.001 compared with the model.

Fig. 2 Examples of model outputs with corresponding ground truth and predictions of nonexpert anaesthesiologists.

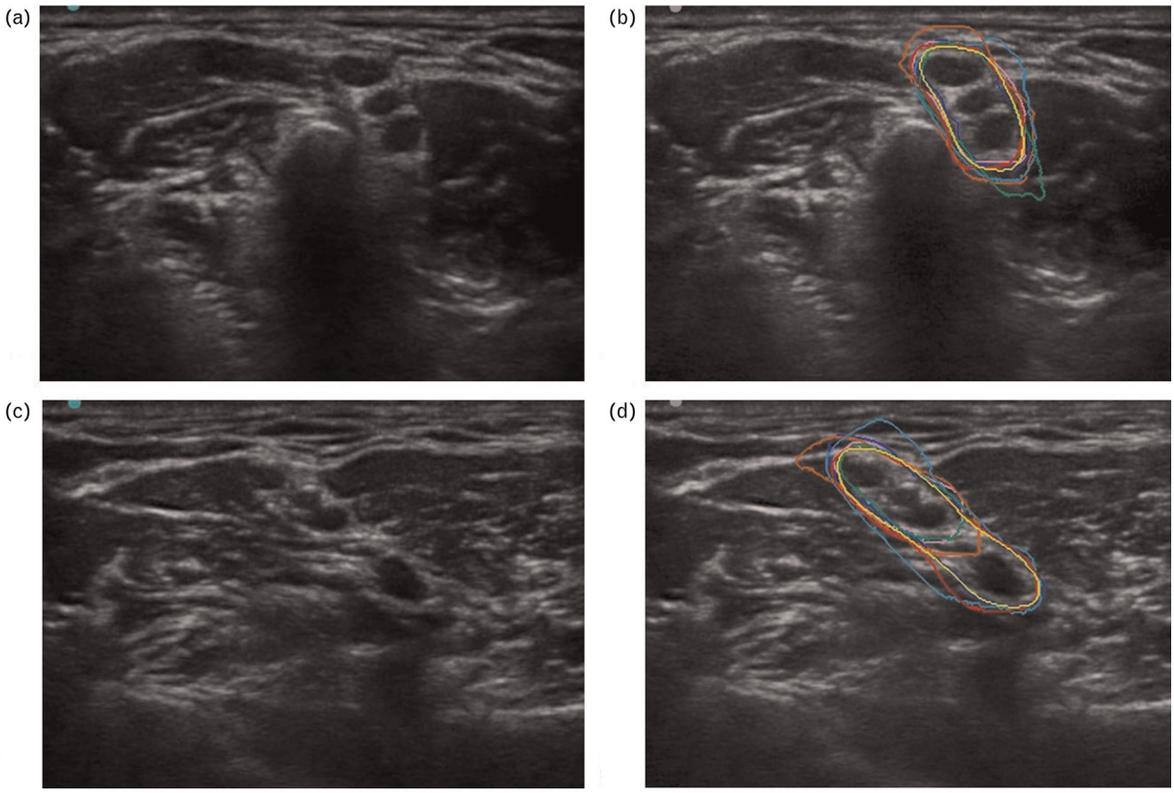

Two examples of ultrasound images (a and c) of the test dataset and the same images (b and d) overlain with the annotations: expert annotation, red; model prediction, yellow; nonexpert anaesthesiologist 1 predictions, blue; nonexpert anaesthesiologist 2, pink; nonexpert anaesthesiologist 3, orange; nonexpert anaesthesiologist 4, sky blue; nonexpert anaesthesiologist 5, green. Intersection over union of image (b): model, 0.839; nonexpert anaesthesiologist 1, 0.763; nonexpert anaesthesiologist 2, 0.843; nonexpert anaesthesiologist 3, 0.689; nonexpert anaesthesiologist 4, 0.690; nonexpert anaesthesiologist 5, 0.696. F1 scores of image (b): model, 0.913; nonexpert anaesthesiologist 1, 0.866; nonexpert anaesthesiologist 2, 0.915; nonexpert anaesthesiologist 3, 0.816; nonexpert anaesthesiologist 4, 0.817; nonexpert anaesthesiologist 5, 0.821. Intersection over union of image (d): model, 0.852; nonexpert anaesthesiologist 1, 0.785; nonexpert anaesthesiologist 2, 0.451; nonexpert anaesthesiologist 3, 0.508; nonexpert anaesthesiologist 4, 0.720; nonexpert anaesthesiologist 5, 0.581. F1 scores of image (d): model, 0.920; nonexpert anaesthesiologist 1, 0.880; nonexpert anaesthesiologist 2, 0.621; nonexpert anaesthesiologist 3, 0.674; nonexpert anaesthesiologist 4, 0.837; nonexpert anaesthesiologist 5, 0.409.

studies. Furthermore, these training images were carefully annotated by a group of expert anaesthesiologists and the model was tested on an independent data set. On the basis of these reasons, our trained model has surpassed the previous models in locating nerves.

The precise detection of nerve boundaries is important for both the success and the safety of nerve blocks.[25] Incorrect recognition of nerve boundaries may lead to inadvertent intraneural or subepineural needle placement, thereby increasing the risk of nerve injury.[26] A cadaver study of ultrasound guided in-plane interscalene block revealed that unintentional injection within the epineurium might occur with a rate as high as 50%, much more frequent than previously estimated.[27] Our results support this assumption as there was a significant variation in the identification of the brachial plexus nerve sheath by the five nonexpert anaesthesiologists (Fig. 2, Supplemental Figure 8, http://links.lww.com/EJA/A746). Another cadaver study has demonstrated that, apart from the increased incidence of direct neural injury, subepineural injection within the interscalene brachial plexus can result in epidural spread of dye.[28] In our study at the C6 level, the median auto-recognition error at the lateral side of the brachial plexus boundary was less than 1 mm. Whether such imprecision is clinically acceptable needs further study.

We suggest that our nerve location model has the potential to augment the ability of nonexpert anaesthesiologists to discern targeted nerves. There were many misidentifications of the elements of the brachial plexus in annotations by nonexpert anaesthesiologists. The most common mistakes were identifying parts of a nerve root surrounded by fascicles as an entire nerve or mistaking a nerve root as an entire cord. These mistakes suggest that even qualified anaesthesiologists can hardly maintain the necessary competence when only

occasionally performing a specific nerve block in their clinical practice. At present, our model can only work with static images, therefore, a feasible clinical use would be taking a 'snapshot' of the real-time ultrasound screen and evaluating the image using the artificial intelligence model. The processing time for an extracted still image through the network is approximately 800 ms, indicating that the artificial intelligence network could be used in a near real-time system of nerve identification. By providing a 'second opinion', the model might assist in reducing human error where expert advice is not readily available, for example, in primary care and rural hospitals. Further studies are needed to verify these assumptions.

There are several limitations in this study. First, the study was conducted at a single medical centre and had a limited data size. The inclusion of retrospective data might also add bias to the analysis. Therefore, our results may not be fully generalisable to other institutions, different populations and operating conditions. Extensive external validation is needed to further assess the performance of the model, especially comparisons between the model and expert anaesthesiologists to evaluate its overall potential to help anaesthesiologists during regional anaesthesia. It is also conceivable that, with additional data inputs, the performance of our model has the potential to improve continuously. Second, the model and nonexpert anaesthesiologists were compared in an experimental setting. Locating nerves in a single ultrasound image may not fully represent the ability of anaesthesiologists to identify the nerves: in a clinical scenario of interscalene block, anaesthesiologists can confirm the location of the brachial plexus by adjusting image settings or tracking nerves along their courses back into the cervical spine. Finally, we used manual expert annotations as accurate when defining the ground truth.

Conclusion

In conclusion, we have demonstrated that computer artificial intelligence based on a deep learning approach can locate the interscalene brachial nerves in ultrasound images with better accuracy than nonexpert anaesthesiologists.

Acknowledgements relating to this article

Assistance with the study: the authors sincerely thank Kai-Lin Xu, MD, Jing-Jing Dong, MD, Yi-Die Su, MD, Zhou-Jing Yang, MD, Ning-Jing Ding, MD, Shan-Shan Zheng, MD, Ting-Ting Wang, MD, Xia-Min Yang, MD for their indispensable help during data collection, Ming-Cheng Li, BS, for his devoted guidance and support on computer techniques, Ye-Hua Cai, MD, for his excellent expert advices on sonography during the study and Professor Wei Zhang, PhD, for his kind and generous help in statistical analysis.

Financial support and sponsorship: this work was supported by National Natural Science Foundation, People's Republic of China (81671058 and 81730031 to YWW); and the Foundation of Shanghai Municipal Key Clinical Specialty (shslczdzk06901 to YWW).

Conflicts of interest: none.

Presentation: none.

References

1 Bailey CR, Ahuja M, Bartholomew K, *et al.* Guidelines for day-case surgery 2019: guidelines from the Association of Anaesthetists and the British Association of Day Surgery. *Anaesthesia* 2019; **74**:778–792.
2 Brattwall M, Jildenstål P, Warrén Stomberg M, *et al.* Upper extremity nerve block: how can benefit, duration, and safety be improved? An update. *F1000Res* 2016; **5**:; F1000 Faculty Rev:907.
3 Helen L, O'Donnell BD, Moore E. Nerve localization techniques for peripheral nerve block and possible future directions. *Acta Anaesthesiol Scand* 2015; **59**:962–974.
4 Marhofer P, Harrop-Griffiths W, Willschke H, *et al.* Fifteen years of ultrasound guidance in regional anaesthesia: part 2-recent developments in block techniques. *Br J Anaesth* 2010; **104**:673–683.
5 Hsu PC, Chang KV, Mezian K, *et al.* Sonographic pearls for imaging the brachial plexus and its pathologies. *Diagnostics (Basel)* 2020; **10**:324.
6 Orebaugh SL, Williams BA. Brachial plexus anatomy: normal and variant. *ScientificWorldJournal* 2009; **28**:300–312.
7 Chandra A, Eisma R, Felts P, *et al.* The feasibility of micro-ultrasound as a tool to image peripheral nerves. *Anaesthesia* 2017; **72**:190–196.
8 Liu SS, YaDeau JT, Shaw PM, *et al.* Incidence of unintentional intraneural injection and postoperative neurological complications with ultrasound-guided interscalene and supraclavicular nerve blocks. *Anaesthesia* 2011; **66**:168–174.
9 Hadjerci O, Hafiane A, Makris P, *et al.* Nerve detection in ultrasound images using median gabor binary pattern. ICIAR 2014, Part II, LNCS 8815. Edited by Campilho A, Kamel M. Switzerland, Springer International Publishers, 2014, pp. 132–140.
10 Hafiane A, Vieyres P, Delbos A. Phase-based probabilistic active contour for nerve detection in ultrasound images for regional anaesthesia. *Comput Biol Med* 2014; **52**:88–95.
11 Smistad E, Iversen DH, Leidig L, *et al.* Automatic segmentation and probe guidance for real-time assistance of ultrasound-guided femoral nerve blocks. *Ultrasound Med Biol* 2017; **43**:218–226.
12 Connor CW. Artificial intelligence and machine learning in anesthesiology. *Anesthesiology* 2019; **131**:1346–1359.
13 Lakhani P, Sundaram B. Deep learning at chest radiography: automated classification of pulmonary tuberculosis by using convolutional neural networks. *Radiology* 2017; **284**:574–582.
14 Zhang J, Gajjala S, Agrawal P, *et al.* Fully automated echocardiogram interpretation in clinical practice. *Circulation* 2018; **138**:1623–1635.
15 Budmuma N. Chapter 5. Convolutional neural networks.*Fundamentals of deep learning*. USA: O'Reilly Media Inc; 2017; 85–116.
16 Topol EJ. High-performance medicine: the convergence of human and artificial intelligence. *Nat Med* 2019; **25**:44–56.
17 Nam JG, Park S, Hwang EJ, *et al.* Development and validation of deep learning-based automatic detection algorithm for malignant pulmonary nodules on chest radiographs. *Radiology* 2019; **290**:218–228.
18 Plante T, Rontes O, Bloc S, *et al.* Spread of local anesthetic during an ultrasound-guided interscalene block: does the injection site influence diffusion? *Acta Anaesthesiol Scand* 2011; **55**:664–669.
19 Yeghiazaryan V, Voiculescu I. Family of boundary overlap metrics for the evaluation of medical image segmentation. *J Med Imaging (Bellingham)* 2018; **5**:015006.
20 Attia ZI, Kapa S, Lopez-Jimenez F, *et al.* Screening for cardiac contractile dysfunction using an artificial intelligence-enabled electrocardiogram. *Nat Med* 2019; **25**:70–74.
21 Gurovich Y, Hanani Y, Bar O, *et al.* Identifying facial phenotypes of genetic disorders using deep learning. *Nat Med* 2019; **25**:60–64.
22 Mori Y, Kudo SE, Misawa M, *et al.* Real-time use of artificial intelligence in identification of diminutive polyps during colonoscopy: a prospective study. *Ann Intern Med* 2018; **169**:357–366.

23 Huang C, Zhou Y, Tan W, *et al.* Applying deep learning in recognizing the femoral nerve block region on ultrasound images. *Ann Transl Med* 2019; **7**:453.
24 Smistad E, Johansen KF, Iversen DH, *et al.* Highlighting nerves and blood vessels for ultrasound-guided axillary nerve block procedures using neural networks. *J Med Imaging (Bellingham)* 2018; **5**:044004.
25 O'Donnell BD, Loughnane F. Novel nerve imaging and regional anesthesia, bio-impedance and the future. *Best Pract Res Clin Anaesthesiol* 2019; **33**:23–35.
26 Neal JM. Ultrasound-guided regional anesthesia and patient safety: update of an evidence-based analysis. *Reg Anesth Pain Med* 2016; **41**:195–204.
27 Orebaugh SL, McFadden K, Skorupan H, *et al.* Subepineurial injection in ultrasound-guided interscalene needle tip placement. *Reg Anesth Pain Med* 2010; **35**:450–454.
28 Fritsch G, Hudelmaier M, Danninger T, *et al.* Bilateral loss of neural function after interscalene plexus blockade may be caused by epidural spread of local anesthetics: a cadaveric study. *Reg Anesth Pain Med* 2013; **38**:64–68.